



Cite this: *Dalton Trans.*, 2024, **53**, 5249

Preparation of silyl-terminated branched polyethylenes catalyzed by Brookhart's nickel diimine complex activated with hydrosilane/B(C₆F₅)₃†

Vojtech Varga, Kristýna Pokorná, Martin Lamač, Michal Horáček and Jiří Pinkas  *

Brookhart's nickel α -diimine complex $[(\kappa_2-N,N\text{-BIAN})\text{NiCl}_2]$ (1) (where BIAN = {Ar=N=Ace=N-Ar}, Ace = acenaphthen-1,2-diyl, and Ar = 2,6-(iPr)₂-C₆H₃) activated with a hydrosilane/B(C₆F₅)₃ (SiHB) adduct forms a highly active catalytic system for ethylene polymerization. Under optimal conditions, the activity of the system depends on the nature of hydrosilane and decreases in the order R₃SiH > Ph₂SiH₂ > PhSiH₃. The decrease in system activity within the hydrosilane series is correlated with increasing formation of Ni(i) species. In addition to their activation effect, hydrosilanes act as efficient chain termination/chain transfer agents, with the Si/Ni ratio controlling the molecular weight of the resulting polyethylene (PE). The use of Et₃SiH generated elastomeric, highly branched polymers with a saturated chain-end, while systems using Ph₂SiH₂ and PhSiH₃ led to branched end-functionalized PEs terminated with the hydrosilyl functionality (i.e. br-PE-SiPh₂H or br-PE-SiPhH₂).

Received 14th December 2023,
Accepted 13th February 2024

DOI: 10.1039/d3dt04200f
rsc.li/dalton

Introduction

Brookhart's discovery of nickel and palladium α -diimine complexes and their use for chain-walking ethylene polymerization stands as one of the milestones of modern polyolefin chemistry.¹ The specific mechanism led to the formation of branched polyethylenes (br-PEs) from homopolymerization of ethylene. The importance of the catalyst and thereof produced materials has been highlighted in several recent reviews.^{2,3} Most works were focused on the modification of the ligand structure of the parent nickel complex to increase its activity and stability; however, the investigation of the role of co-catalysts/activators is rather scarce. Since the initial discovery, methylaluminoxane (MAO) and its derivatives remained the most utilized co-catalysts for the activation of nickel-halide bonds. Unlike early transition metal complexes, organoaluminium compounds (R₂AlCl and RAlCl₂, where R = Me, Et) are also efficient in activating nickel diimine dihalide complexes at low Al/Ni ratios.^{4–7}

Silane-functionalized polyolefins (Si-PO) have been explored for their unique properties and possible utilization as compatibilizers for blending the polyolefin with inorganic fillers, processing

aids and battery separators.⁸ The Si-PO polymers could be prepared by various methods, for example post-functionalization of vinyl-terminated polyolefins (e.g. hydrosilylation), free radical grafting, and coordination polymerization (Chart 1). Coordination polymerization was mainly used for the preparation of branched PO (particularly br-PE). In this respect, Brookhart explored the copolymerization of ethylene with vinyltrialkoxysilanes using nickel and palladium α -diimine complexes to produce silyl-functionalized br-PEs. The copolymerization afforded low to medium (5–60 branches per 1000C, Ni catalyst) and highly branched (100 branches per 1000C, Pd catalyst) copolymers with multiple trialkoxysilyl groups incorporated.^{9,10} Later on, Chen extended the methodology to the copolymerization of ethylene with *in situ* generated allylsilanes to produce polyolefin bearing silyl-functionalized branches.¹¹

Another strategy for the introduction of the silane functionality as the PE end-group was developed by Marks.¹² The strategy used hydrosilanes as chain transfer agents (CTAs); however, it was applied mostly for lanthanide and early transition metal catalysts and produced mainly linear silyl-terminated PEs.¹³ Recently, the catalyst scope was extended to late transition metal complexes based on cobalt and palladium by Guironnet, and the latter gave rise to end-functionalized silyl-terminated br-PEs.^{14,15} Guironnet proposed a mechanism where the formation of species having metal–silicon bonds is the key point of the catalytic cycle. Subsequently, ethylene is inserted into the M–Si bond (and then repeatedly into the M–

J. Heyrovský Institute of Physical Chemistry, Academy of Sciences of the Czech Republic, v.v.i., Dolejškova 3, 182 23 Prague 8, Czech Republic.

E-mail: jiri.pinkas@jh-inst.cas.cz

† Electronic supplementary information (ESI) available. See DOI: <https://doi.org/10.1039/d3dt04200f>



Silicon-functionalized Branched Polyolefins

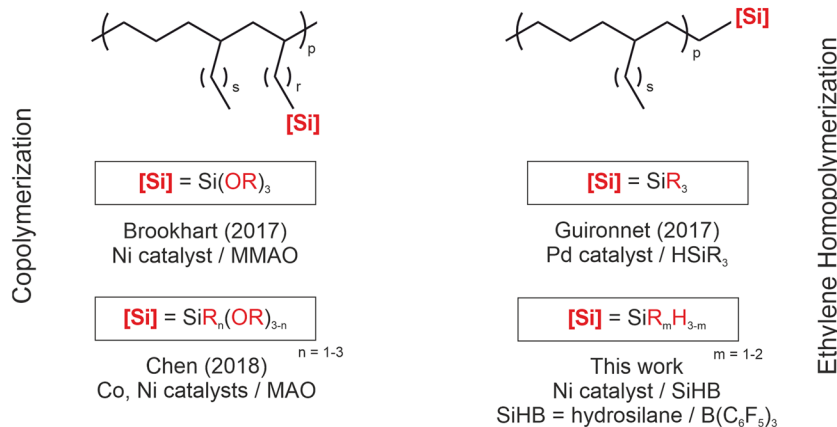


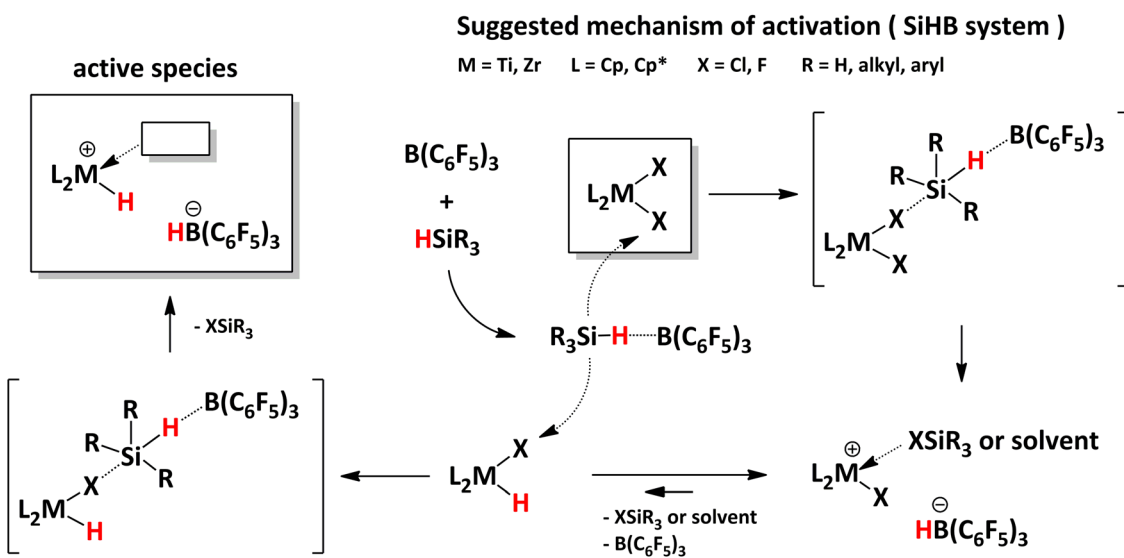
Chart 1 Branched Si-PO and their preparation.

polymeryl bond) and the cycle is looped by termination with hydrosilane. The hydride is transferred from hydrosilane to the polymer chain and M-Si species is regenerated. It should be mentioned that the last step (hydride transfer to polymer) is consistent with the observations made by Brookhart, where using Et_3SiH for the cleavage of neutral Pd-alkyl or cationic Pd-polyolefinyl generated a saturated alkane/polyolefin.^{16,17} On the other hand, the cleavage of Ni-octyl bonds in the nickel diimine complex with hydrosilanes $\text{HSiMe}_n(\text{OEt})_{3-n}$ ($n = 0-3$) resulted in the respective 1-octylsilanes as shown by Chirik.¹⁸

In recent years, we have investigated the hydrosilane/ $\text{B}(\text{C}_6\text{F}_5)_3$ (SiHB) system for the activation of early transition (Ti, Zr) metal halide complexes to generate catalytic systems for

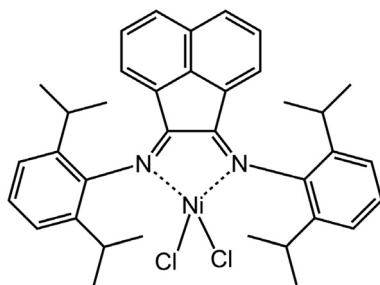
catalytic (co)polymerization of olefins and hydrodehalogenation reactions.¹⁹⁻²² We proposed that the hydride transfer from hydrosilane to $\text{B}(\text{C}_6\text{F}_5)_3$ and finally to the transition metal is the key activation step (Scheme 1).

Herein, we extend the utilization of the SiHB system to late-transition metal complexes. We describe the activation of Brookhart's nickel α -diimine complex $[(\kappa_2\text{-}N,N\text{-BIAN})\text{NiCl}_2]$ (1), where BIAN = {Ar-N=Ace=N-Ar}, Ace = acenaphthen-1,2-diyl and Ar = 2,6-(iPr)₂-C₆H₃ (Chart 2), with SiHB and use thereof generated system in the chain-walking polymerization of ethylene. We demonstrate the importance of the hydrosilane nature and the Si/Ni molar ratio in the system activity and the resulting polymer structure. In addition, we show the first example of the preparation of hydrosilyl-terminated br-PEs.



Scheme 1 Proposed SiHB system activation mechanism.



Chart 2 Brookhart's nickel α -diimine complex **1**.

Results and discussion

Performance of $1/B(C_6F_5)_3$ /hydrosilane in ethylene polymerization

We started the investigation with a tertiary silane using the $1/B(C_6F_5)_3/Et_3SiH$ system based on our previous results with zirconocene precatalysts.^{19,23} We proposed that a hydride transfer from the hydrosilane to the boron center and finally to a transition metal has general validity and could be applied to **1** as well. The catalytic system based on **1** showed comparable activity but a different reaction profile (represented by ethylene uptake, Fig. S1 in ESI[†]) in comparison to the $Cp_2ZrCl_2/B(C_6F_5)_3/Et_3SiH$ system under similar conditions.²³ We noted a steady kinetics during the initial state of the polymerization catalyzed by the active species derived from **1**, probably as a result of the active species stability and lower sensitivity to impurities. In a series of preliminary experiments (Table 1), we determined conditions to achieve an optimal catalytic efficiency and a reproducible polymerization outcome as follows: concentration of $[1] = 0.1\text{ mM}$ (*i.e.* 5 μmol per 50 ml), $\text{Si}/\text{B}/\text{Ni} = 3000/3/1$, and dichloromethane was used as the solvent. Under these conditions, the system reached activities 3180 and 3130 $\text{kg}_{\text{PE}}\text{ (mol}_{\text{Ni}}\text{ h bar})^{-1}$, respectively (entries 3 and 4 in Table 1), while utilization of toluene as the polymerization medium led to *ca.* half activity (1460 $\text{kg}_{\text{PE}}\text{ (mol}_{\text{Ni}}\text{ h bar})^{-1}$, entry 5 in Table 1). Notably, ethylene solubility under the given conditions is quite similar for toluene (0.4 M)²⁴ and dichloro-

methane (0.5 M);²⁵ therefore, we suggest that this does not contribute to the difference in system activity. The lower ethylene polymerization activity in toluene is in agreement with considerably slower 1-hexene polymerization in toluene-*d*₈ in comparison to CD_2Cl_2 observed during NMR experiments (see below). The best activities obtained with the $1/B(C_6F_5)_3/Et_3SiH$ system are *ca.* 25% lower in comparison to those obtained for $1/\text{MMAO}$ in CH_2Cl_2 by us (4070 $\text{kg}_{\text{PE}}\text{ (mol}_{\text{Ni}}\text{ h bar})^{-1}$, entry 8 in Table 1) or for $1/\text{MAO}$ in toluene by Brookhart (4340 $\text{kg}_{\text{PE}}\text{ (mol}_{\text{Ni}}\text{ h bar})^{-1}$).¹ At lower concentrations of **1**, (entries 6 and 7 in Table 1), we also obtained activities close to those for MAO activation; however, the reproducibility of polymerization was considerably lower.

Subsequently, we investigated the effect of the Si/Ni molar ratio (the studied range of the Si/Ni ratio was 10–6000) on the system performance and produced polymer properties. The results are summarized in Table 2. Interestingly, the system showed some activity even at the lowest studied Si/Ni ratios of 10 and 50 (entries 1 and 2 in Table 2), giving activities 25 and 980 $\text{kg}_{\text{PE}}\text{ (mol}_{\text{Ni}}\text{ h bar})^{-1}$, respectively. This indicates the applicability of the $Et_3SiH/B(C_6F_5)_3$ activator system at a low Si/Ni ratio, similar to the activation of $[(\kappa_2-N,N\text{-BIAN})\text{NiBr}_2]$ with the organoaluminium activator Et_2AlCl (where the Al/Ni ratio was as low as 10).^{4,5} The reasonable activity of the system at low Si/Ni ratios could also be explained by the higher tolerance of the system towards impurities (low electrophilicity and oxophilicity of the active species derived from **1** in comparison to group 4 complexes). A further increase in the Si/Ni ratio from 100 to 3000 (entries 3–6, Table 2) led to higher system activity, reaching its maximum value of 3180 $\text{kg}_{\text{PE}}\text{ (mol}_{\text{Ni}}\text{ h bar})^{-1}$ at $\text{Si}/\text{Ni} = 3000$. At the highest Si/Ni ratio of 6000 (entry 7, Table 2), a *ca.* 25% activity drop to 2730 $\text{kg}_{\text{PE}}\text{ (mol}_{\text{Ni}}\text{ h bar})^{-1}$ was observed, while ethylene consumption was lower in comparison to entry 6 during the whole polymerization process (Fig. S2 in ESI[†]). This could be attributed to the lower amount of active species due to their reduction to inactive $\text{Ni}(\text{i})$ species (see below).

Generally, we suggest the presence of stable active species during the polymerization at a wide Si/Ni range (50–6000) for up to five minutes (prolonged polymerization times are substantially hampered by reactor fouling even at $\text{Si}/\text{Ni} = 50$),

Table 1 Ethylene polymerization results of $1/B(C_6F_5)_3$ /hydrosilane catalytic systems. Catalyst optimization experiments^a

Entry	Ni (μmol)	Polym. medium	Si/B/Ni	T (min)	P (bar)	Yield (g)	A^b	M_n^c (g mol^{-1})	M_w/M_n^c	Bran. per 1000C ^d
1 ^e	15	CH_2Cl_2	1000/1	1	3	1.916	2550	67 800	1.9	
2	5	CH_2Cl_2	3000/3	5	1	1.314	3150	49 600	3.4	
3	5	CH_2Cl_2	3000/3	5	3	3.980	3180	47 500	3.3	71
4 ^f	5	CH_2Cl_2	3000/3	5	3	3.910	3130			
5 ^g	5	TOL	3000/3	5	3	1.830	1460	81 200	2.9	
6	2.5	CH_2Cl_2	3000/3	5	3	2.408	3850	85 200	3.4	
7	1	CH_2Cl_2	3000/3	5	3	0.940	3760	143 100	2.7	
8	1	CH_2Cl_2	MMAO, Al/Ni (1000/1)	10	3	2.036	4070	229 900	2.1	
Ref. 1	0.83	TOL	MAO, Al/Ni (1000/1)	30	1	1.800	4340	190 000	2.2	70

^a Polymerization conditions: **1** was dissolved in CH_2Cl_2 , hydrosilane was Et_3SiH , temperature 25 °C, total volume 50 mL, rpm 800. ^b $[A] = \text{kg}_{\text{PE}}\text{ (mol}_{\text{Ni}}\text{ h bar})^{-1}$. ^c Determined by HT-SEC. ^d Determined by NMR. ^e Very high initial activity (ethylene consumption 900 mL min^{-1} after 10 s), highly exothermic (temperature jumps to 50 °C within 1 min), mass transport problem. ^f Reproducibility experiment to entry 3. ^g Serious mass transport and diffusion problem, after 2 min a jellylike material was observed (no PE precipitation).



Table 2 Ethylene polymerization catalyzed with **1/B(C₆F₅)₃/tertiary silane** systems^a

Entry	Silane	Si/Ni	T (min)	Yield (g)	A ^b	M _n ^c (g mol ⁻¹)	M _w /M _n ^c	Bran. per 1000C ^d	T _m ^e (°C)	X _c ^e (%)
1	Et ₃ SiH	10	30	0.190	25	177 500	2.5		81	22
2	Et ₃ SiH	50	5	1.230	980	138 200	2.9		71	19
3	Et ₃ SiH	100	5	1.890	1510	130 600	2.8		63	15
4	Et ₃ SiH	500	5	2.673	2140	95 800	3.3		54	11
5 ^f	Et ₃ SiH	1500	5	3.302	2640	80 500	3.1		47	9
6 ^f	Et ₃ SiH	3000	5	3.980	3180	47 500	3.3	71	28	5
7 ^f	Et ₃ SiH	6000	5	3.413	2730	73 100	2.8		11	5
8	Me ₂ PhSiH	3000	5	2.525	2020	22 900	4.7	60	64	14
9	(EtO) ₃ SiH	3000	10	1.085	430	124 400	3.2		73	18

^a Polymerization conditions: [1] = 0.1 mM, polymerization medium CH₂Cl₂, temperature 25 °C, pressure 3 bar, B/Ni = 3, total volume 50 mL, rpm 800. ^b [A] = kg_{PE} (mol_{Ni} h bar)⁻¹. ^c Determined by HT-SEC. ^d Determined by NMR. ^e Determined by DSC from the second heat. ^f Ethylene mass transport problem.

which was supported by ethylene consumption profiles (Fig. S2 in the ESI†). However, at the highest Si/Ni ratios (3000 and 6000) a drop in the ethylene consumption could be observed as polymerization matured (after *ca.* 3–4 min). This was a result of reactor fouling and ethylene diffusion limitation.

In addition to Et₃SiH, we have tested other tertiary silanes: Me₂PhSiH (entry 8, Table 2, A = 2020 kg_{PE} (mol_{Ni} h bar)⁻¹) and (EtO)₃SiH (entry 9, Table 2; A = 430 kg_{PE} (mol_{Ni} h bar)⁻¹); however, the respective catalytic systems were considerably less active in comparison to Et₃SiH.

Next, we tested secondary (Ph₂SiH₂) and primary (PhSiH₃) silanes in the activation of **1** at Si/Ni ratios of 10–3000 (Table 3). Ph₂SiH₂ was able to activate **1** at the lowest Si/Ni ratio of 10, giving activities 3 times higher (85 kg_{PE} (mol_{Ni} h bar)⁻¹, entry 1 in Table 3) in comparison to Et₃SiH (25 kg_{PE} (mol_{Ni} h bar)⁻¹, entry 1 in Table 2) under the same conditions. Further increasing the Si/Ni ratio to 100 led to a maximum activity of the **1/B(C₆F₅)₃/Ph₂SiH₂** system (300 kg_{PE} (mol_{Ni} h bar)⁻¹, entry 3 in Table 3); however, this value is *ca.* one order of magnitude lower in comparison to the maximum values obtained for the system activated with Et₃SiH. Interestingly, further increasing the Si/Ni ratio led to systems with decreased

activity, with the lowest value obtained at the highest Si/Ni ratio of 3000 (15 kg_{PE} (mol_{Ni} h bar)⁻¹, entry 5 in Table 3).

The inhibiting effect of excessive silane was even more pronounced when we used PhSiH₃. At the lowest Si/Ni ratio of 10, we obtained a *ca.* 6-times more active system (155 kg_{PE} (mol_{Ni} h bar)⁻¹, entry 6 in Table 3) in comparison to **1/B(C₆F₅)₃/Et₃SiH** under the same conditions. Further increasing the Si/Ni ratio led to a decrease in the **1/B(C₆F₅)₃/PhSiH₃** system activity and finally resulted in a complete system inactivity at Si/Ni 3000 (entry 9 in Table 3). The drop in activity with increasing PhSiH₃/**1** ratio is accompanied by a significant color change of the polymerization mixture: yellow (PhSiH₃/**1** = 10), brown (PhSiH₃/**1** = 50), greenish (PhSiH₃/**1** = 100), and green (PhSiH₃/**1** = 3000).

Binary hydrosilane Et₃SiH/Ph₂SiH₂ system

The inhibiting effect of excessive silane (particularly secondary and tertiary ones) was further investigated in polymerization experiments involving a binary silane system (Table 4).

The addition of a small amount of Ph₂SiH₂ to the most effective system **1/B(C₆F₅)₃/Et₃SiH** (Et₃SiH/Ph₂SiH₂ ratio 60) led to a deterioration of the system activity to *ca.* one half (1900 kg_{PE} (mol_{Ni} h bar)⁻¹, entry 1 in Table 4) in comparison

Table 3 Ethylene polymerization catalyzed with **1/B(C₆F₅)₃/Ph₂SiH₂** or PhSiH₃^a

Entry	Silane	Si/Ni	T (min)	Yield (g)	A ^b	Si per 1000C ^c	Si ^{d,e} (mol%)	M _n ^f (g mol ⁻¹)	M _w /M _n ^f	Bran. per 1000C ^e	T _m ^g (°C)	X _c ^g (%)
1	Ph ₂ SiH ₂	10	30	0.635	85	n. o. ^h		163 100	2.7		79	20
2	Ph ₂ SiH ₂	50	5	0.270	220	0.243	52	30 200	3.4		85	23
3	Ph ₂ SiH ₂	100	5	0.370	300	0.537	56	14 600	3.0		86	27
4	Ph ₂ SiH ₂	500	5	0.175	140	3.028	67	3100	2.8		89	24
5	Ph ₂ SiH ₂	3000	30	0.110	15	n. d. ⁱ		1200	1.5	40	69	28
6	PhSiH ₃	10	30	1.165	155	n. o. ^h		48 100	3.4	45	82	23
7	PhSiH ₃	50	30	0.476	65	0.509	13	3700	2.8		88	30
8	PhSiH ₃	100	30	0.370	50	0.837	11	1900	2.4	37	91	30
9	PhSiH ₃	3000	30	0	0							

^a Polymerization conditions: [1] = 0.1 mM, polymerization medium CH₂Cl₂, temperature 25 °C, pressure 3 bar, B/Ni = 3, total volume 50 mL, rpm 800. ^b [A] = kg_{PE} (mol_{Ni} h bar)⁻¹. ^c Determined by FT-IR (pressed foils, transmission mode). ^d Percentage of silyl terminated polymers.

^e Determined by NMR. ^f Determined by HT-SEC. ^g Determined by DSC from the second heat. ^h n. o. signal corresponding to the Si–H stretch was not observed (or is beyond the spectrometer's resolution capability). ⁱ Not determined (waxy material, unsuitable for foil preparation), ATR ZnSe shows very high Si content.



Table 4 Ethylene polymerization catalyzed with $1/B(C_6F_5)_3$ /binary silane systems^a

Entry	Silane	Si/Ni	T (min)	Yield (g)	A^b	M_n^c (g mol ⁻¹)	M_w/M_n^c	T_m^d (°C)	X_c^d (%)
1	Et_3SiH	3000	5	2.370	1900	21 800	2.5	64	13
	Ph_2SiH_2	50							
2	Et_3SiH	3000	30	0.204	30	1100	1.5	71	28
	Ph_2SiH_2	3000							

^a Polymerization conditions: $[1] = 0.1$ mM; solvent CH_2Cl_2 ; temperature 25 °C; pressure 3 bar; $B/Ni = 3$; total volume 50 mL; rpm 800. ^b $A = kg_{PE}$ ($mol_{Ni} h bar$)⁻¹. ^c Determined by HT-SEC. ^d Determined by DSC from the second heat.

to the Et_3SiH system (3180 kg_{PE} ($mol_{Ni} h bar$)⁻¹). Further increasing the Ph_2SiH_2 amount to an equimolar ratio with Et_3SiH (total Si/Ni 6000, entry 2, Table 3) led to an activity collapse to an about 2-orders lower value of 30 kg_{PE} ($mol_{Ni} h bar$)⁻¹. After isolation of the polymer, the polymerization mixture (entry 2) was concentrated and analyzed by GC-MS (Fig. S3†). No ethylene oligomers (either Si-modified or not), products of hydrosilane dehydrocoupling or products of ethylene hydrosilylation/dehydrogenative silylation were detected.

Polymer characterization

Obtained polymers were analyzed by high-temperature size exclusion chromatography (HT-SEC), DSC, and IR (ATR) and selected ones were analyzed by NMR spectroscopy (results are summarized in Tables 1–4). The polymer properties depended particularly on the hydrosilane nature and the Si/Ni ratio used for the activation.

The polymers produced from tertiary silane activation were obtained as elastomeric materials with low melting points and low crystallinity. ¹H NMR of selected examples showed a branched structure (70 and 60 branches per 1000C) typical of Brookhart's catalyst.³

In addition, ¹H NMR and FT-IR spectroscopy confirmed the presence of a saturated chain end, although a trace amount (<1%) of olefinic chain ends was also detected (see Fig. S4 and S6 in the ESI†). Et_3SiH efficiently terminated the polymer growth, whereas the Si/Ni ratio controlled the M_n of the produced polymers. Steadily increasing the Si/Ni ratio from 10 to 6000 decreased the M_n from 177 500 to 22 900 Da. The presence of a saturated chain end raised suspicion about the termination of the polymer chain with H_2 generated by Et_3SiH dehydrocoupling. However, we were unable to detect any disilane $Et_3SiSiEt_3$ in the polymerization mixture despite several attempts. Therefore, this pathway could be excluded and further investigation is necessary. Notably, the utilization of Et_3SiH for the modulation of the M_n of the produced PEs (to *ca.* half at Si/Ni 2000) during nickel diimine derivatives/MAO system catalysis was already patented.²⁶ In addition, the cleavage of Pd^+ -polymethyl bonds with Et_3SiH was used for the precise generation of saturated-end polymers by Brookhart.¹⁷ Therefore, we suggest that tertiary silanes acted as chain termination agents, controlling the M_n of the produced br-PE in the 1/SiHB system.

The polymers formed from systems utilizing Ph_2SiH_2 and $PhSiH_3$ showed higher melting points and crystallinity in com-

parison to the ones prepared with Et_3SiH . This reflects their lower branch content (37–45 branches per 1000C), whereas a similar relationship was mentioned for branched polyolefins.²⁷ We suggest that lower branching may be connected with enhanced formation of Ni(i) species upon activation of 1 with Ph_2SiH_2 and $PhSiH_3$ as shown by EPR experiments (see the section "Activation study using EPR spectroscopy"). Similarly, about 30% decrease in branching was observed when the Ni(ii) diimine precatalyst was reduced to Ni(i) species with $CoCp_2$ prior to MAO activation.²⁸

Polyolefin M_n values were negatively affected by an increasing Si/Ni ratio, too. The highest M_n values were obtained at lowest Si/Ni = 10 (163 100 Da for Ph_2SiH_2 – entry 1 in Table 3; 48 100 Da for $PhSiH_3$ – entry 6 in Table 3) and the lowest M_n values were obtained at the highest Si/Ni ratio (*i.e.* 1200 Da for $Ph_2SiH_2/Ni = 3000$ – entry 5 in Table 3; 1900 Da for $PhSiH_3/Ni = 100$ – entry 8 in Table 3). Unlike Et_3SiH (and other tertiary hydrosilanes), Ph_2SiH_2 and $PhSiH_3$ acted as CTAs and generated end-functionalized PEs having a considerable amount of polymer chains (11–67 mol%) terminated with the silyl functionality. Moreover, the dependence of polyethylene M_n on the reciprocal diphenylsilane concentration is practically linear and indicates that Ph_2SiH_2 is an effective CTA under the given conditions (Fig. 1). The presence of terminal $-SiPh_2H$ (Fig. 2) and $-SiPhH_2$ (Fig. S5 in ESI†) was unequivocally proved by ¹H NMR and ATR spectroscopy.

The properties of the polymers generated from binary Et_3SiH/Ph_2SiH_2 systems were significantly affected by the presence of Ph_2SiH_2 . The polymer number average molecular

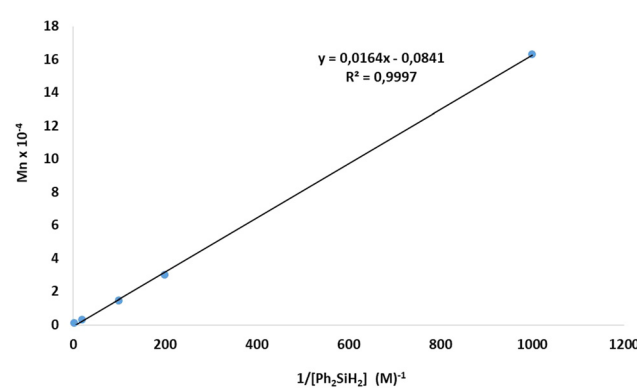


Fig. 1 The dependence of the polymer M_n (entries 1–5 in Table 3) on $1/[Ph_2SiH_2]$.



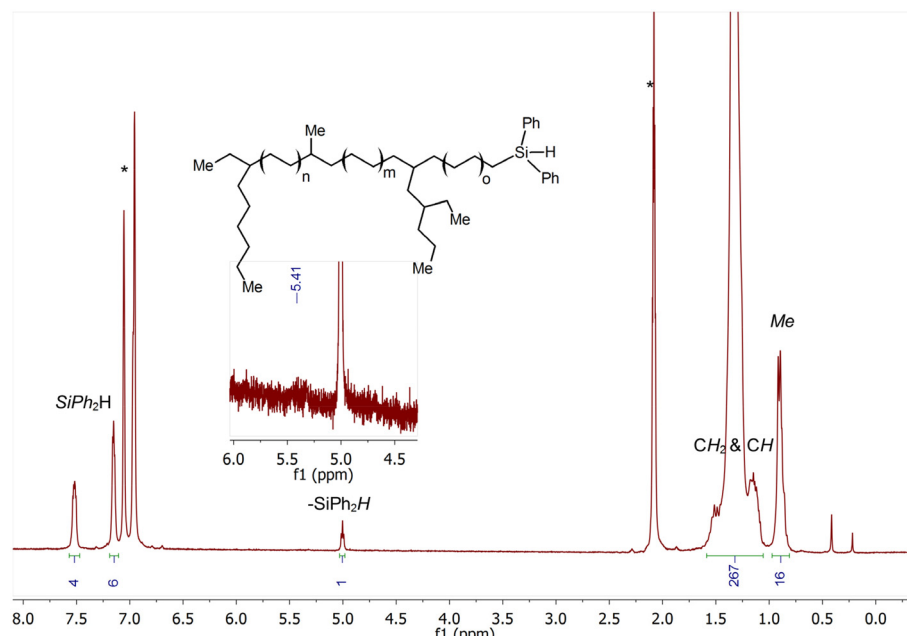


Fig. 2 ^1H NMR spectrum of br-PE-SiPh₂H (entry 5 in Table 3) recorded at 100 °C in toluene- d_8 . (*) denotes the residual proton signals of the solvent. The inset spectrum indicates a trace amount of internal double bonds in the polymer (multiplet centered at 5.41 ppm).

weight (M_n) was reduced to one half in comparison to that produced with sole Et₃SiH (21 800 Da for entry 1 in Table 4 vs. 47 500 Da for entry 6 in Table 2) even at a low Ph₂SiH₂ content (Et₃SiH/Ph₂SiH₂ ratio of 60). At an equimolar hydrosilane ratio, the M_n of the prepared polymer was very similar to the one prepared with sole Ph₂SiH₂ (1100 Da for entry 2 in Table 4 vs. 1200 Da for entry 5 in Table 3). In addition, the polymer is terminated with -SiPh₂H similar to what was found for polymers prepared with sole Ph₂SiH₂ (for IR spectra of the polymers, see Fig. S7 in the ESI†).

Mechanistic NMR experiments

The paramagnetic nature of **1** hampered the detailed investigation of catalytic species using NMR spectroscopy; however, it gives some information about other components of the catalytic system (hydrosilane, B(C₆F₅)₃, olefin). In a series of experiments, we investigated the reactions of **1**/B(C₆F₅)₃/hydrosilane in the presence/absence of 1-hexene in either CD₂Cl₂ or toluene- d_8 .

The addition of excess 1-hexene to a mixture of **1**/B(C₆F₅)₃/10 eq. Et₃SiH in CD₂Cl₂ led to an instant 1-hexene polymerization. The ^1H NMR spectrum of the mixture, recorded immediately after sample preparation, showed only polymeric material (its formation was also supported by $^{13}\text{C}\{^1\text{H}\}$ NMR), while no 1-hexene was detected at all (Fig. S8 in ESI†). In addition to Et₃SiH ($\delta_{\text{Si}} = -0.4$), the formation of Et₃SiCl was detected in ^{29}Si NMR spectra ($\delta_{\text{Si}} = 36.6$). ^{11}B and ^{19}F NMR spectra showed a mixture of B(C₆F₅)₃ and [HB(C₆F₅)₃]⁻, while broad signals in ^{19}F NMR indicated a dynamic exchange between the species.

The analogous reaction in the absence of 1-hexene showed also the formation of Et₃SiCl and [HB(C₆F₅)₃]⁻ as deduced from multinuclear NMR. However, we also observed the for-

mation of Et₃SiF (Fig. S9 in the ESI† doublet at $\delta_{\text{Si}} = 32.9$ ppm, $\delta_{\text{F}} = -176.0$ ppm), which supported the generation of strongly electrophilic species (as B(C₆F₅)₃ and [HB(C₆F₅)₃]⁻ are the only sources of fluoride). Notably, the EPR spectroscopy of the sample showed the presence of Ni(i) species (for details, see below). Aging of the sample led to the gradual replacement of the Et₃SiH signals with Et₃SiCl signals (completed within 7 days) and the formation of CD₂ClH and CD₂H₂ (Fig. S10 in the ESI†) from CD₂Cl₂. This implies the potency of the **1**/B(C₆F₅)₃/hydrosilane system for dehalogenation catalysis, similar to what was published for the group 4 complexes/B(C₆F₅)₃/hydrosilane system.²²

The polymerization of 1-hexene (using the **1**/B(C₆F₅)₃/10 eq. Et₃SiH system) in toluene- d_8 in a sealed NMR tube proceeded only sluggishly in comparison to that conducted in CD₂Cl₂. ^1H NMR showed only 5% of polyolefin after 4 days, while full conversion was obtained after 2 months (Fig. 3). The $^{29}\text{Si}\{^1\text{H}\}$ NMR spectrum acquired after 2 months showed Et₃SiCl ($\delta_{\text{Si}} = 35.3$ ppm) and unreacted Et₃SiH ($\delta_{\text{Si}} = -0.1$ ppm) (Fig. S11 in ESI†) as the only silicone species. This excludes many processes potentially taking place with the system (e.g. 1-hexene hydrosilylation, Et₃SiH dehydrocoupling, etc.). The ^1H NMR spectrum (Fig. 3c) showed the presence of internal double bonds (multiplet 5.34–5.44); however, the signals consist of mixture of 2- and 3-hexenes as supported by $^{13}\text{C}\{^1\text{H}\}$ (Fig. S12 in ESI†) and 2D NMR experiments. The isolated polyolefin lacks any considerable olefinic signals either in ^1H (Fig. 3d) or $^{13}\text{C}\{^1\text{H}\}$ (Fig. S12 in ESI†) NMR spectra. This supports our assumption that β -H elimination is not a significant chain termination process with the catalytic system using **1**/B(C₆F₅)₃/tertiary hydrosilane.



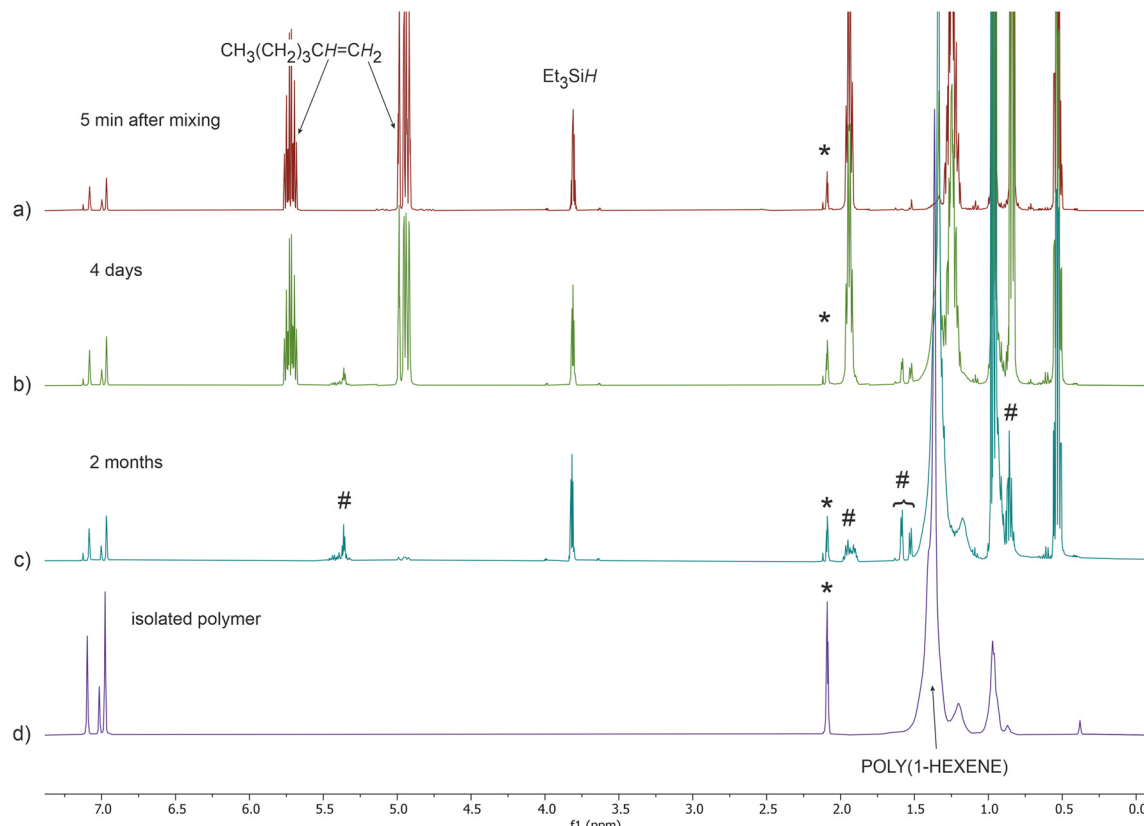


Fig. 3 ^1H NMR spectrum of mixture 1/B(C₆F₅)₃/100 eq. Et₃SiH/200 eq. 1-hexene in toluene-*d*₈ recorded 5 min (a), 4 days (b), and 2 months (c) after mixing. For comparison, poly(1-hexene) isolated from the experiment (d). Signals corresponding to the mixture of 2- and 3-hexenes are marked (#).

Activation study using EPR spectroscopy

The utilization of a high Si/Ni ratio for the activation of **1** led to a lower or no system activity, while the effect of excessive silane inhibition was increased in the order $\text{Et}_3\text{SiH} < \text{Ph}_2\text{SiH}_2 < \text{PhSiH}_3$. This could be rationalized either as a competitive coordination of excessive silane to an active center or reduction of $\text{Ni}^{(\text{II})}$ species to inactive/dormant $\text{Ni}^{(\text{I})}$ ones.

The formation of Ni(I) species during the activation of nickel α -diimine complexes with aluminium activators (like MAO, MMAO and alkylaluminium species) has been repeatedly mentioned in the literature.²⁹⁻³² To follow and understand the SiHB activation processes associated with the oxidation state changes of the nickel center, EPR experiments using three hydrosilanes were performed. The detailed experimental setup and conditions are described in the ESI.†

The equimolar mixture of **1** and $B(C_6F_5)_3$ was found to be EPR silent for more than 40 min. However, after the addition of 10 equivalents of any of the studied hydrosilanes (Et_3SiH , Ph_2SiH_2 , and $PhSiH_3$), we observed the formation of two signals in the EPR spectrum within a few minutes: a broad singlet signal ($\Delta H = 40$ G) at $g = 2.132$ and a 7-lined signal at g value 2.001 with hyperfine splitting $a = 5.1$ G (Fig. 4A). The formation of a Ni(i) species in the presence of a SiHB system is proposed to be responsible for the first signal, while an

organic radical positioned at the BIAN anion could be responsible for the second signal (for detailed discussion, see the ESI†). The intensity of the organic radical is not significantly affected by the nature of the hydrosilane; therefore, we suggest that the species is not involved in a catalytic cycle. On the other hand, the intensity of the Ni(i) species is significantly affected by the nature of the hydrosilane and increased in the order $\text{Et}_3\text{SiH} < \text{Ph}_2\text{SiH}_2 < \text{PhSiH}_3$. Cooling the samples to 123 K (toluene glass) led to an anisotropic EPR spectrum with axial symmetry exhibiting resonances with two g -values: $g_{\parallel} = 2.233$ and $g_{\perp} = 2.070$ (Fig. 4B). The Ni(i) species with the same EPR parameters ($g_{\text{iso}} = 2.132$, $g_{\parallel} = 2.234$, $g_{\perp} = 2.070$) were mentioned in the literature as products of AlMe_3 activation ($\text{Ni/Al} = 1/100$) of $[(\kappa_2-N,N\text{-BIAN})\text{NiBr}_2]$ – a bromide analogue of **1**, where the authors suggested the formation of heterobinuclear Ni(i) species having two bridging methyl groups $[(\kappa_2-N,N\text{-BIAN})\text{Ni(i)(}\mu\text{-Me)}_2\text{AlMe}_2]$.^{29,31} In the present case, the absence of aluminum compounds and the presence of borane $\text{B}(\text{C}_6\text{F}_5)_3$ and hydrosilane in the SiHB activation system led us to suggest the possible structure of the observed Ni(i) species as a cationic Ni(i) complex (Chart 3) accompanied by a hydridoborate anion, where S denotes any coordinating species (solvent, hydrosilane, chlorosilane, or hydridoborate). The presence of a neutral monochloride or monohydride complex is less likely due to the formation of a dimeric structure, which was

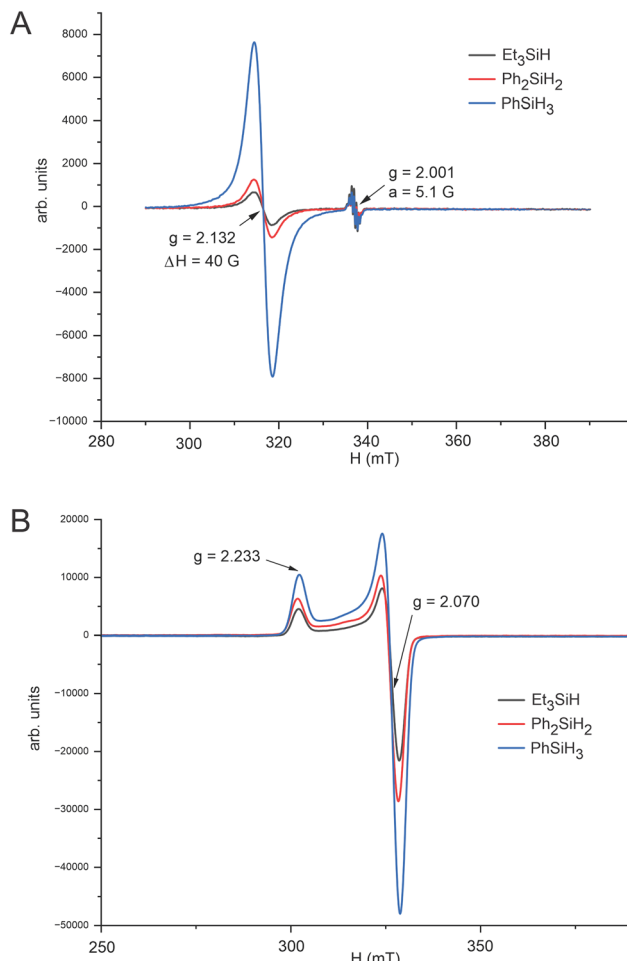


Fig. 4 Comparison of the EPR spectra of the mixture $1/\text{B}(\text{C}_6\text{F}_5)_3/10$ eq. hydrosilane recorded 5 min after hydrosilane addition at 297 K (A) and the spectra recorded again at 113 K after 3 h (B). $[\text{Ni}] = 6.5 \mu\text{M}$, toluene.

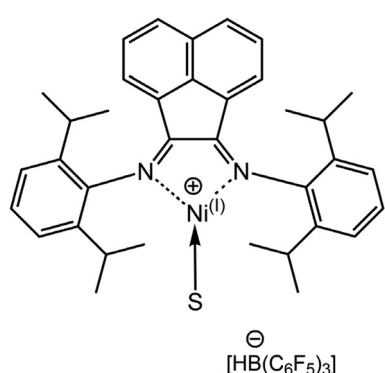


Chart 3 Proposed structure of the $\text{Ni}^{(i)}$ species generated during the activation of **1** with the SiHB system.

reported in the literature^{33–36} The absence of Ni–alkyl or Ni–H bonds in the proposed $\text{Ni}^{(i)}$ species precludes an olefin insertion; therefore, it could not be reactivated as was mentioned for the $[(\kappa_2\text{-}N,N\text{-BIAN})\text{Ni}^{(i)}(\mu\text{-Me})_2\text{AlMe}_2]$ species.

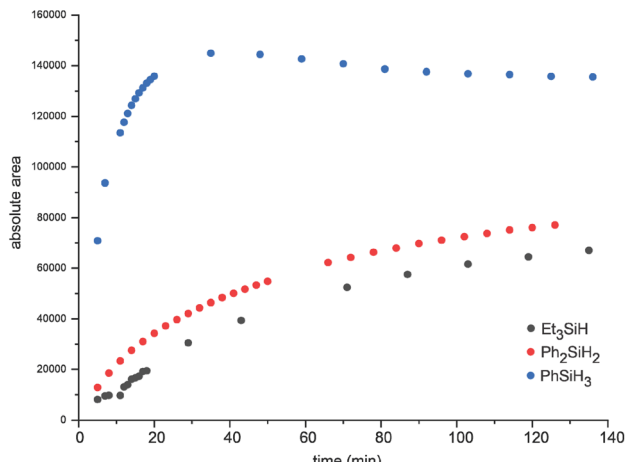


Fig. 5 Time evolution of the $\text{Ni}^{(i)}$ signal in the $1/\text{B}(\text{C}_6\text{F}_5)_3/10$ eq. hydrosilane mixture.

To verify the inertness of the $\text{Ni}^{(i)}$ species, 1-hexene was added to the mixture $1/\text{B}(\text{C}_6\text{F}_5)_3/10$ eq. Et_3SiH ; however, no change of the $\text{Ni}^{(i)}$ EPR signal was registered within several days (see Fig. S13 in the ESI†). This is in agreement with the fact that the “naked” cationic species are catalytically inactive for ethylene polymerization, as reported by Gao.³³ It should be mentioned that poly(1-hexene) was isolated from the mixture after 5 days, which supports the presence of an active species (the EPR silent one) in the mixture. These observations led us to the conclusion that the $\text{Ni}^{(i)}$ species formed during the activation of **1** with the SiHB system is catalytically inactive rather than a “dormant” one.

In the next step, we followed the $\text{Ni}^{(i)}$ signal intensity time evolution in $1/\text{B}(\text{C}_6\text{F}_5)_3/10$ eq. hydrosilane (for Et_3SiH , Ph_2SiH_2 , PhSiH_3) systems at standard **1** concentration. The results (Fig. 5) supported the increasing reducing ability of the SiHB system in the order $\text{Et}_3\text{SiH} < \text{Ph}_2\text{SiH}_2 < \text{PhSiH}_3$. The maximum $\text{Ni}^{(i)}$ level was reached with PhSiH_3 after 35 minutes, while other hydrosilanes did not reach a plateau.

It should be mentioned that the positive effect of $\text{Ni}^{(i)}$ species on lowering the branching of PE was recently mentioned by Roy.²⁸ As the lower branching content in PEs prepared by Ph_2SiH_2 and PhSiH_3 was observed during our studies, a further detailed EPR investigation involving secondary and primary hydrosilanes is necessary.

Conclusion

We have extended the applicability of the SiHB system as an alternative (aluminium-free) activator for late transition metal complexes using Brookhart's nickel α -diimine derivative **1**. This system is capable of generating catalytically active species for ethylene polymerization with activities comparable to the **1/MAO** system. The catalytic activity is controlled by the nature of hydrosilane (the activity decreases in the order tertiary silane $>$ Ph_2SiH_2 $>$ PhSiH_3) and the Si/Ni ratio. Based on EPR



experiments, we propose that the decrease in activity could be associated with the increasing formation of inactive $\text{Ni}(\text{i})$ species. The M_n of the generated medium to highly branched PEs could be efficiently modulated by the nature of hydrosilane and the Si/Ni ratio, which demonstrated the chain transfer ability of all hydrosilanes used. However, we have found differences in the chain transfer process depending on the hydrosilane used. The utilization of tertiary hydrosilanes led to PEs with saturated chain-ends, while using Ph_2SiH_2 and PhSiH_3 generated end-functionalized br-PEs terminated with the hydrosilyl functionality.

Consequently, this is the first example of end-functionalized br-PEs prepared with Brookhart-type nickel catalysts. The presence of the reactive hydrosilane functionality at the polymer chain-end is particularly attractive as it allows post-modification of the polymer (*e.g.* oxidation to silanol function) and its grafting with other materials.

In addition to olefin polymerization, the 1/SiHB system could find applications in hydrodehalogenation, as observed during our NMR experiments. Further investigations of the mechanism of activation, active species deactivation, and polymer chain transfer to hydrosilanes are in progress.

Conflicts of interest

The authors declare no conflicts of interest.

Acknowledgements

This research was supported by the Czech Science Foundation (project 21-01308S). The authors thank Prof. Jan Merna (ICT, Prague) for HT-SEC and DSC measurements of the prepared polymers.

References

- 1 L. K. Johnson, C. M. Killian and M. Brookhart, *J. Am. Chem. Soc.*, 1995, **117**, 6414.
- 2 F. Wang and C. Chen, *Polym. Chem.*, 2019, **10**, 2354.
- 3 R. K. Wu, W. K. Wu, L. Stieglitz, S. Gaan, B. Rieger and M. Heuberger, *Coord. Chem. Rev.*, 2023, **474**, 214844.
- 4 D. Pappalardo, M. Mazzeo and C. Pellecchia, *Macromol. Rapid Commun.*, 1997, **18**, 1017.
- 5 J. C. W. Chien, S. Fernandes, S. G. Correia, M. D. Rausch, L. C. Dickson and M. M. Marques, *Polym. Int.*, 2002, **51**, 729.
- 6 J. M. Rose, A. E. Cherian and G. W. Coates, *J. Am. Chem. Soc.*, 2006, **128**, 4186.
- 7 J. Peleska, Z. Hostalek, D. Hasalikova and J. Merna, *Polymer*, 2011, **52**, 275.
- 8 Y. Q. Cai, W. Y. Fang, J. Y. Zheng, J. Xu and H. Fan, *Can. J. Chem. Eng.*, 2023, **1**.
- 9 Z. Chen, W. J. Liu, O. Daugulis and M. Brookhart, *J. Am. Chem. Soc.*, 2016, **138**, 16120.
- 10 Z. Chen, M. D. Leatherman, O. Daugulis and M. Brookhart, *J. Am. Chem. Soc.*, 2017, **139**, 16013.
- 11 S. X. Zhou and C. L. Chen, *Sci. Bull.*, 2018, **63**, 441.
- 12 P. F. Fu and T. J. Marks, *J. Am. Chem. Soc.*, 1995, **117**, 10747.
- 13 S. B. Amin and T. J. Marks, *Angew. Chem., Int. Ed.*, 2008, **47**, 2006.
- 14 M. G. Hyatt and D. Guironnet, *ACS Catal.*, 2017, **7**, 5717.
- 15 M. G. Hyatt and D. Guironnet, *Organometallics*, 2019, **38**, 788.
- 16 A. M. LaPointe, F. C. Rix and M. Brookhart, *J. Am. Chem. Soc.*, 1997, **119**, 906.
- 17 A. C. Gottfried and M. Brookhart, *Macromolecules*, 2001, **34**, 1140.
- 18 I. Pappas, S. Treacy and P. J. Chirik, *ACS Catal.*, 2016, **6**, 4105.
- 19 V. Varga, M. Lamač, M. Horáček, R. Gyepes and J. Pinkas, *Dalton Trans.*, 2016, **45**, 10146.
- 20 V. Varga, M. Večeřa, R. Gyepes, J. Pinkas, M. Horáček, J. Merna and M. Lamač, *ChemCatChem*, 2017, **9**, 3160.
- 21 V. Varga, J. Pinkas, I. Císařová, J. Kubišta, M. Horáček, K. Mach and R. Gyepes, *Eur. J. Inorg. Chem.*, 2018, 2637.
- 22 D. Dunlop, J. Pinkas, M. Horáček, N. Žilková and M. Lamač, *Dalton Trans.*, 2020, **49**, 2771.
- 23 V. Varga, M. Lamač, M. Horáček and J. Pinkas, Method for preparation of silane-modified polyolefins, catalytic system and its utilization, CZ309742, 2023.
- 24 A. L. McKnight and R. M. Waymouth, *Macromolecules*, 1999, **32**, 2816.
- 25 S. Mecking, L. K. Johnson, L. Wang and M. Brookhart, *J. Am. Chem. Soc.*, 1998, **120**, 888.
- 26 S. D. Arthur and S. J. McLain, Molecular weight control in olefin polymerization, US6372869B1, 2002.
- 27 M. Zada, A. Vignesh, L. Guo, R. Zhang, W. Zhang, Y. Ma, Y. Sun and W.-H. Sun, *ACS Omega*, 2020, **5**, 10610.
- 28 R. C. Chapleski, J. L. Kern, W. C. Anderson, B. K. Long and S. Roy, *Catal. Sci. Technol.*, 2020, **10**, 2029.
- 29 I. E. Soshnikov, N. V. Semikolenova, K. P. Bryliakov, A. A. Antonov and E. P. Talsi, *Organometallics*, 2022, **41**, 1015.
- 30 I. E. Soshnikov, N. V. Semikolenova, K. P. Bryliakov and E. P. Talsi, *Catalysts*, 2021, **11**, 1386.
- 31 I. E. Soshnikov, N. V. Semikolenova, K. P. Bryliakov, A. A. Antonov, W. H. Sun and E. P. Talsi, *J. Organomet. Chem.*, 2020, **907**, 121063.
- 32 S. Y. Xu, X. M. Chen, G. Luo and W. Gao, *Dalton Trans.*, 2021, **50**, 7356.
- 33 W. Gao, L. Xin, Z. Hao, G. Li, J.-H. Su, L. Zhou and Y. Mu, *Chem. Commun.*, 2015, **51**, 7004.
- 34 V. V. Khrizanforova, R. R. Fayzullin, V. I. Morozov, I. F. Gilmutdinov, A. N. Lukoyanov, O. N. Kataeva, T. P. Gerasimova, S. A. Katsyuba, I. L. Fedushkin, K. A. Lyssenko and Y. H. Budnikova, *Chem. – Asian J.*, 2019, **14**, 2979.
- 35 N. A. Eberhardt and H. Guan, *Chem. Rev.*, 2016, **116**, 8373.
- 36 Q. S. Dong, Y. X. Zhao, Y. T. Su, J. H. Su, B. A. Wu and X. J. Yang, *Inorg. Chem.*, 2012, **51**, 13162.

